

# Wavelength and Depth of Ribbing in Roll Coating and Its Elimination

**Tomiichi Hasegawa**

Dept. of Mechanical System Engineering, Niigata University, Niigata 950-21, Japan

**Kazunori Sorimachi**

Niigata College of Technology, Niigata 950-21, Japan

*Experiment has been made on ribbing induced on a film coated over a roll surface by a two-roll system: one roll rotated with a speed and the other fixed or rotated with relatively different speeds. The two rolls have the same diameters and are placed parallel with each other by keeping a gap. Test fluids are Newtonian (glycerin/water) and viscoelastic [polyacrylamide (Separan AP30)/glycerin/water] solutions. Wavelength and depth of ribbing are measured by a newly developed technique utilizing an image of a straight bar placed above the roll and reflected on the ribbing film surface. Nondimensionalized wavelength is correlated with capillary number for Newtonian liquids, but higher for dilute Separan solutions and lower for nondilute Separan solutions than for Newtonian liquids. The depth of ribbing increases for dilute Separan solutions with nearly the same value for nondilute Separan solutions as those for Newtonian liquid. This behavior observed for the ribbing seems to have some relation to the existence of a line of vortices that occurs visibly for nondilute Separan solutions in the entrance region of the gap between the rolls. Increase in the ratio of the velocities of two rolls has an effect of increasing both the wavelength and depth of ribbing for glycerine and nondilute Separan solutions, but it has the effect of decreasing them for dilute Separan solutions. Addition of Separan in glycerine solution promotes the generation of ribbing.*

*A string spanned near over the gap to touch the surface of the liquid pool between the gap has the effect of eliminating the ribbing. This is successful in various combinations between the speeds of the two rolls and the diameters of the string.*

## Introduction

Thickness and instability of a liquid film coated over a roll surface in roll coating have been frequently discussed, and it is known that nip (gap) width and capillary number of the liquid used have a deep influence on them (Babchin et al., 1981; Benkreira et al., 1981; Adachi, 1986; Takemura et al., 1987).

Pitts and Greiller (1961) and Savage (1977a,b; 1984) made theoretical studies of the film thickness and the position of meniscus. They predicted a critical condition for the generation of ribbing over the liquid film. The critical condition was also investigated by Mill and South (1967) with an experiment using a two roll system of the same size or different sizes. Appearance of ribbing was studied by Coyle et al. (1990a,b,c) theoretically

and experimentally by changing the rotating direction of the rolls and the nip clearance. These investigations have been mainly concerned with the thickness of the liquid film and the critical condition for generation of ribbing and only a few (Mill and South, 1967; Adachi, 1986) were made on the ribbing itself, especially on the wavelength, although the ribbing provides a direct influence on appearance and quality of products.

In the present study, an experiment is made on ribbing induced on a film coated over a roll surface by means of a two-roll system, one roll rotating and the other fixed or rotated with relatively different velocities. Namely, the wavelength and the depth of ribbing are measured by a newly developed technique utilizing an image made on the ribbing film surface by

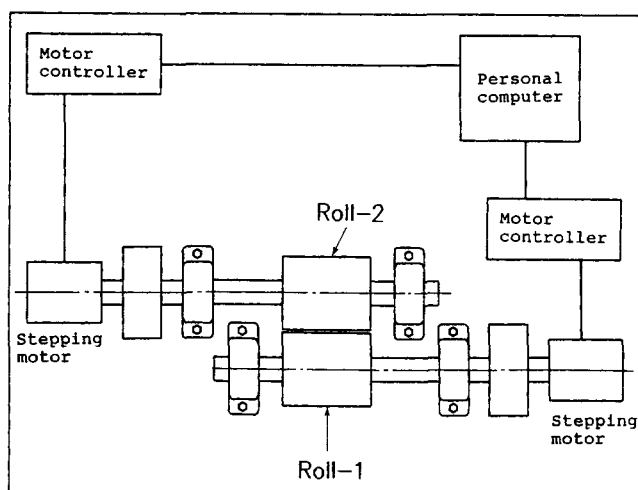


Figure 1. Experimental apparatus.

a reflection of a straight bar placed above the roll. A method to eliminate the ribbing is proposed.

### Experimental Procedure and Apparatus

Experimental apparatus is schematically shown in Figure 1. Both the rolls used were made of stainless steel and have the same radius  $R$  of 40 mm and the same length  $L$  of 100 mm. Gap width  $h$  was of the order of magnitude of 0.1 mm and roll-1 and roll-2 were rotated with a stepping motor with relatively different speeds including the zero speed of roll-1. Figure 2 indicates the detail of the part around the rolls and the experimental procedure. When a liquid possessing an appropriate viscosity is supplied from a reservoir to the V-shaped region surrounded by the roll surfaces over the gap, then the liquid rests for a while in the V-shaped region and a part of the liquid is forced to pass through the gap due to the drag of the surface of the rotating roll. After the pass it forms a thin layer on the surface of the rolls-1 and 2 (the surplus liquid which did not pass through the gap drips down along the side faces of the rolls). See the figure on the right side in Figure 2. In this case, ribbing is produced on the liquid surface according to the condition of rotating speed, gap width, liquid properties, and so on.

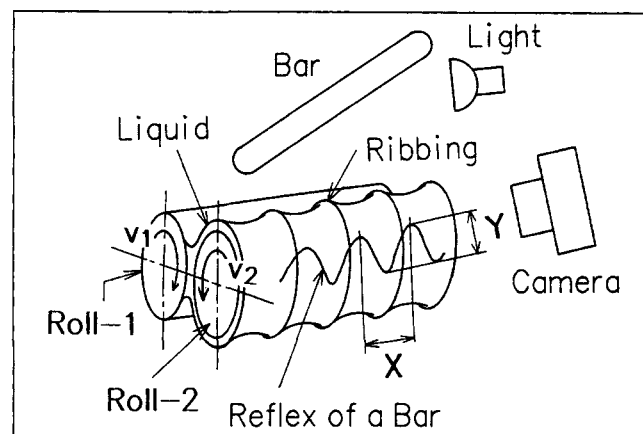


Figure 3. Experimental method for measuring wavelength and depth of the ribbing that occurs on a liquid surface.

The wavelength  $\lambda_2$  and the depth  $h_d$  of thin ribbing (Figures 4, 11-15) were measured by the following procedure (see Figure 3): when a straight bar is placed above the roll and sufficient light is applied, a reflection image of the bar on the liquid film can be observed. This image was photographed and found to be distorted like a sine curve due to the ribbing (see the photographs in Figure 7. When no ribbing occurs, the image is straight and undistorted). It is natural to think that the wavelength  $X$  and the wave magnitude  $Y$  evaluated from the photograph of the image have a relation with the actual wavelength  $\lambda_2$  and depth  $h_d$  of the deformed liquid film. However, the corresponding relation is too difficult to know *a priori* because of the curvature of the roll. Therefore, we took the following experimental approach: thin strings were trapped on the roll with a pitch and a thin vinyl sheet was rapped over the strings so that a false ribbing was produced on the roll, as shown in Figure 5. The pitch  $\lambda_2$  and the depth  $h_d$  of the false ribbing of the vinyl sheet were measured with a touch stylus. Again the reflection image of the false ribbing was photographed and  $X$  and  $Y$  were decided, as in the experiment of the solution. By this procedure, the relations between  $X$  and  $\lambda_2$ , and  $Y$  and  $h_d$  were obtained and this was taken as a calibration curve. Also the wavelength  $\lambda_1$  of the meniscus deformed at the exit of the gap (Figure 6) was measured by taking a photograph of the

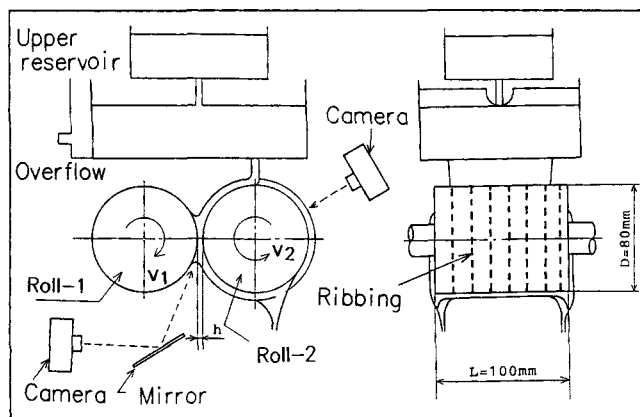


Figure 2. Part of the rolls.

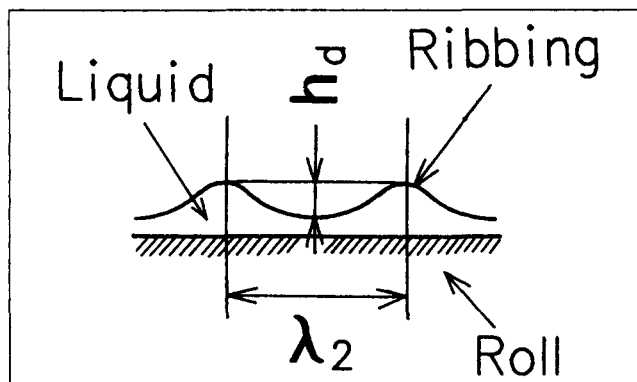


Figure 4. Cross section of the liquid film.

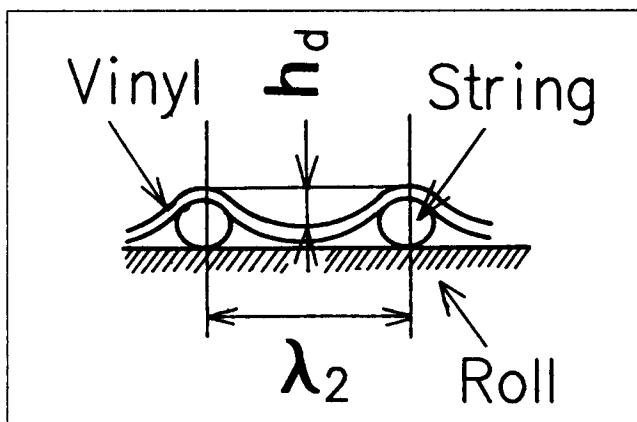


Figure 5. False ribs made by a string and a vinyl sheet.

region by use of a mirror (see Figure 2). Circumference speed  $V_2$  of roll-2 was 0.041, 0.077, 0.132, 0.254 and 0.384 m/s and the gap clearance  $h$  was 0.1 and 0.2 mm. In this case the shear rate at the gap changes from 400 to 4,000  $1/s$  if the fluid velocity is assumed to be linear and roll-1 is stationary. The liquids used are glycerine 80%, 90% solutions in water and syrup 80%, 85% solutions in water as Newtonian fluids and several hundreds ppm of polyacrylamide (Separan AP30) added in glycerine 90% solution in water. Furthermore, to examine the effect of the surface tension, the glycerine 90% and syrup 80% solution in water added by a surfactant APE (polyoxyethylene lauryl ether) was also used. Table 1 gives the liquids used for experiment. The viscosity was measured with a capillary viscometer for a range of shear rate and with a cone-plate viscometer for various temperatures.

## Experimental Result and Discussion

Figure 8 shows the shearing stress,  $\tau$  (Pa) against the shear rate,  $\dot{\gamma}$  ( $s^{-1}$ ) in log-log plots. We see that  $\tau$  has a gradient of

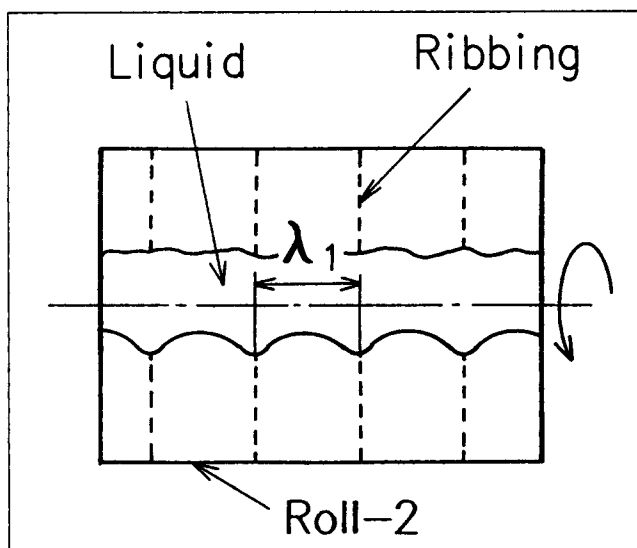


Figure 6. Meniscus at the gap.

Table 1. Liquids Used

No.	Glycerin/ Syrup/Water ratio (%)	Separan (ppm)	PEO (ppm)	APE (%)	Surface Tension $\times 10^{-3}$ N/m ( $^{\circ}$ C)
1	100/-/0				66.2 (12.5)
2	95/-/5				66.3 (12.7)
3	90/-/10				66.9 (12.9)
4	90/-/10			1.6	26.1 (12.9)
5	/85/15				81.2 (13.8)
6	-/80/20				82.4 (25.5)
7	-/80/20			1.3	30.7 (12.9)
8	90/-/10	50			68.7 (15.2)
9	90/-/10	100			68.4 (16.0)
10	90/-/10	200			68.5 (21.1)
11	90/-/10	500			67.4 (21.0)
12	90/-/10	750			67.8 (16.0)
13	90/-/10	1,000			68.1 (10.1)

unity against  $\dot{\gamma}$ , which means Newtonian viscosity of the fluids tested. Also, the viscosity increases as the concentration increases, for instance, the viscosity of glycerine 100% is 10 times higher than that of 90% glycerine solution in water. Figure 9 gives the result of the measurement of the viscosity  $\eta$  Pa·s against the temperature  $\theta^{\circ}$ C with the constant shear rate of  $1.9 s^{-1}$ , where  $\eta$  decreases with temperature and increases with concentration as expected. Wavelength  $\lambda_2$  and depth  $h_d$  of the false ribbing are plotted in Figure 10 respectively against  $X$  and  $Y$  obtained by photographs. Though the data are sparse, we can get calibration curves by taking the least-square method; a straight line for the relation between  $\lambda_2$  and  $X$ , a parabola for  $h_d$  and  $Y$ . These curves are used as calibration curves from which  $\lambda_2$  and  $h_d$  are decided for the liquid film. Values of  $\lambda_2$  obtained for the real liquid film are given in Figures 11, 12a and 12b in the case when  $V_1 = 0$ , where  $\lambda_2$  is made dimensionless with  $(Rh^2)^{1/3}$  and described as  $\lambda_2^*$  and the horizontal line is capillary number  $Ca$ . Considerable scatter is seen in the data in Figure 11 and Figure 13 for  $h_d$  which will be given later. This may be caused partly by the flow instability in the region between the rolls and the temperature increase of the rolls by giving a light for photography or partly by ambiguity in determining  $h_d$  because of some width of the reflection image (see Figure 7). Consequently, the data may have an error around 30%.

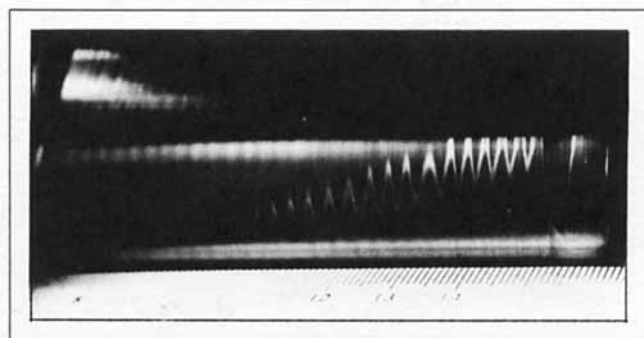
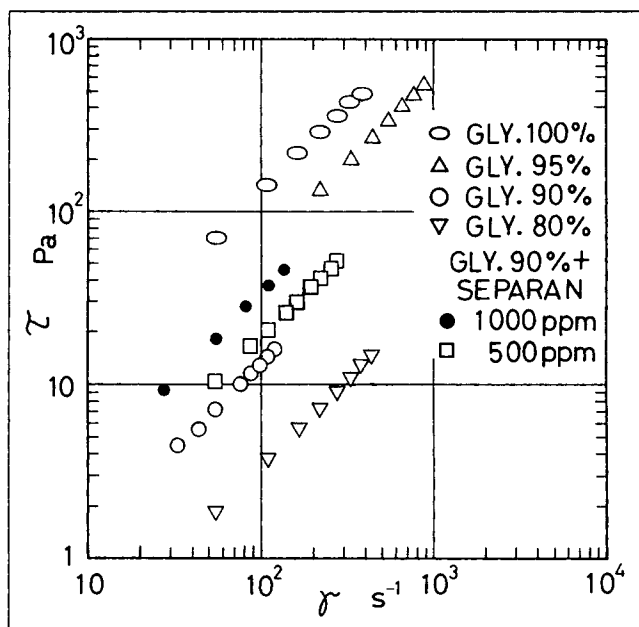
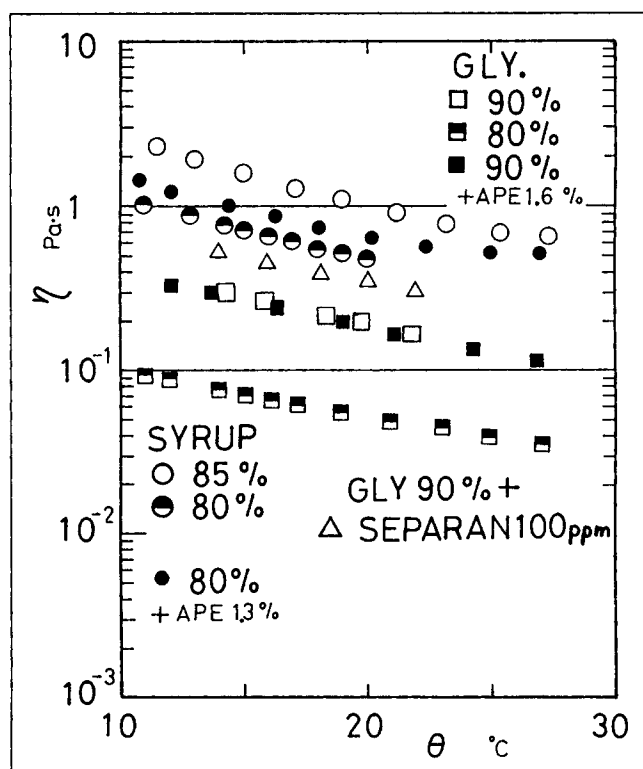


Figure 7. Ribbing, glycerine 90% + Separan 100 ppm solution ( $V_1 = 0$ ,  $V_2 = 0.384$  m/s,  $h = 0.1$  mm).



**Figure 8.** Shearing stress  $\tau$  (Pa) vs. shear rate  $\dot{\gamma}$  ( $\text{s}^{-1}$ ), (measuring temperature is  $\circ$  19°C,  $\Delta$  17°C,  $\circ$  26°C,  $\nabla$  28°C,  $\bullet$  29°C,  $\square$  30°C).

We see in Figure 11 that  $\lambda_2^*$  for Newtonian fluids, except that of syrup 85% solution in water, nearly correlates with  $Ca$  and it has a tendency to reduce with increase of  $Ca$ . In the same figure, Mill and South's data (Mill and South, 1967)



**Figure 9.** Effect of temperature  $\theta$  ( $^{\circ}\text{C}$ ) on the viscosity  $\eta$  ( $\text{Pa}\cdot\text{s}$ ).

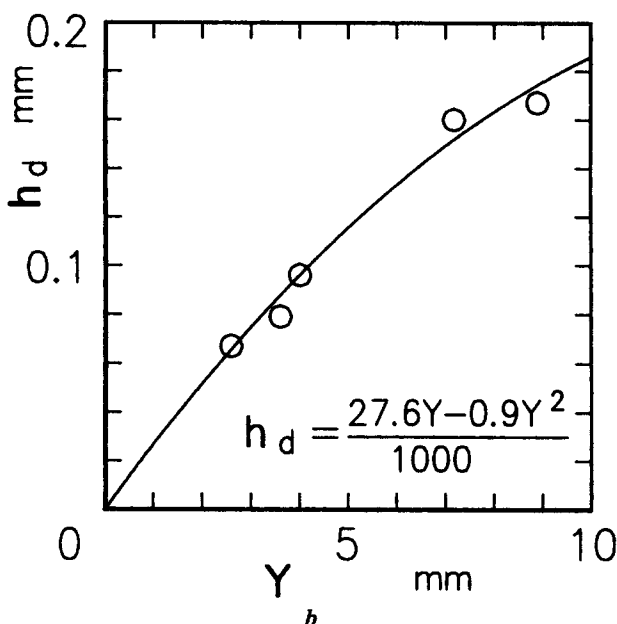
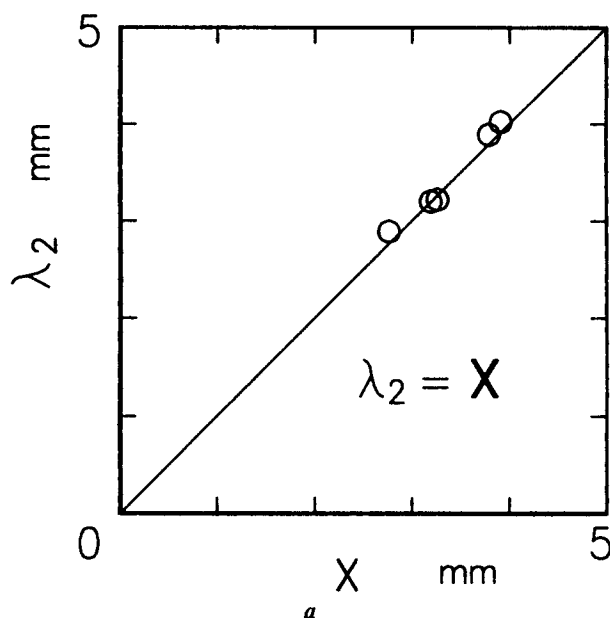


**Figure 10.** Calibration curves of (a) the wavelength  $\lambda_2$  (mm) and (b) the depth  $h_d$  (mm) of ribbing.

obtained for a roll-roll system are shown by a solid line (indicated as R-R), and also an experimental result obtained with a roll-plate system (Adachi, 1986) is shown with a dotted line (indicated as R-P). It is seen that Mill and South's data coincide with the present ones, though the experimental condition is different, and  $\lambda_2^*$  of the roll-plate system has a similar tendency as the present ones but the absolute value.

$\lambda_2^*$  vs.  $Ca$  is given in Figure 12a and Figure 12b for dilute Separan solutions (namely the concentration is less than 200 ppm) and for nondilute Separan solutions (the concentration is more than 500 ppm), respectively. It is seen that  $\lambda_2^*$  is larger for dilute Separan solutions, but smaller for nondilute Separan solutions than that of Newtonian liquids.

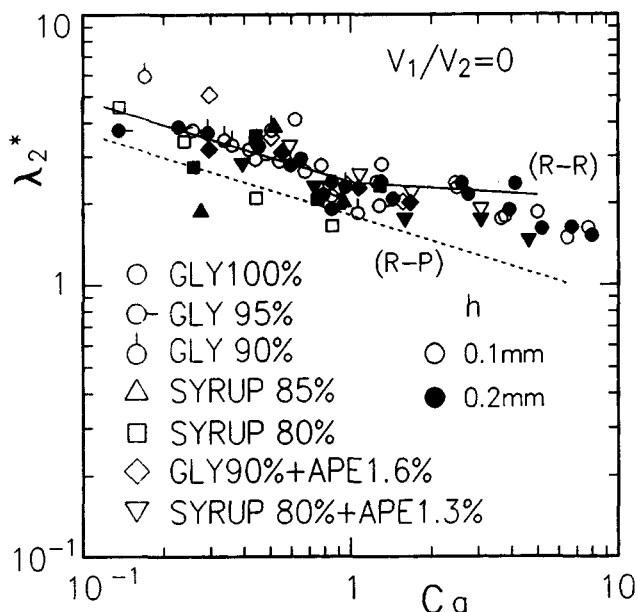


Figure 11. Dimensionless wavelength  $\lambda_2^*$  of ribbing vs. capillary number  $Ca$  for Newtonian liquids.

$h_d$  is presented against  $Ca$  in Figure 13a–13g where it is not dimensionless. One might think that  $h_d$  too should be made dimensionless as  $\lambda_2^*$ , this being easy of course, but it is held as it is because  $h_d$  has been unfamiliar and it is better to know the magnitude directly from the figure. We see that  $h_d$  for glycerine solutions falls in the range of 0.1 to 0.05 mm under the condition of the present experiment, while it increases for dilute Separan solutions but gives lower values for nondilute Separan solutions.

Thus the effect of addition of polymers in glycerine solutions is not simple, but we can discern between dilute and nondilute Separan solutions in the data of  $\lambda_2^*$  and  $h_d$ . Concerning this, it was observed that a line of vortices occurs in the upstream region of the gap for nondilute solutions (see Figure 14b) but no vortex for glycerine and dilute solutions (Figure 14a). These vortices may have some connection to the behavior of  $\lambda_2$  and  $h_d$ , but the details are not clarified yet.

In Figure 15,  $\lambda_2^*$  and  $h_d$  are given for the case when the relative velocity ratio of the two rolls  $V_1/V_2$  is increased. We see both of  $\lambda_2^*$  and  $h_d$  have a similar tendency: the condition that  $V_1/V_2 \neq 0$  increases both values of  $\lambda_2^*$  and  $h_d$  for glycerine 100% (a, d), decreasing them especially in the high range of  $Ca$  for glycerine 90% + Separan 100 ppm solution (b, e), and apparently making them higher for glycerine 90% + Separan 750 ppm solution (c, f).

These effects are shown in Figure 16, in which change in forms of the ribbing with increase of Separan concentration is schematically and exaggeratedly given together with presentation of the existence of vortex for the cases of zero and nonzero rotation of roll 1. Figure 17 indicates a correlation between  $\lambda_1^* [= \lambda_1/(Rh^2)^{1/3}]$  and  $\lambda_2^*$ , where  $\lambda_1$  is the wavelength of the wave-like deformed meniscus occurring at the gap exit in the direction of the axis of the rolls (Figure 6). The data are somewhat scattered, but equivalence is seen between the two and we will be able to say that the wave of the deformed

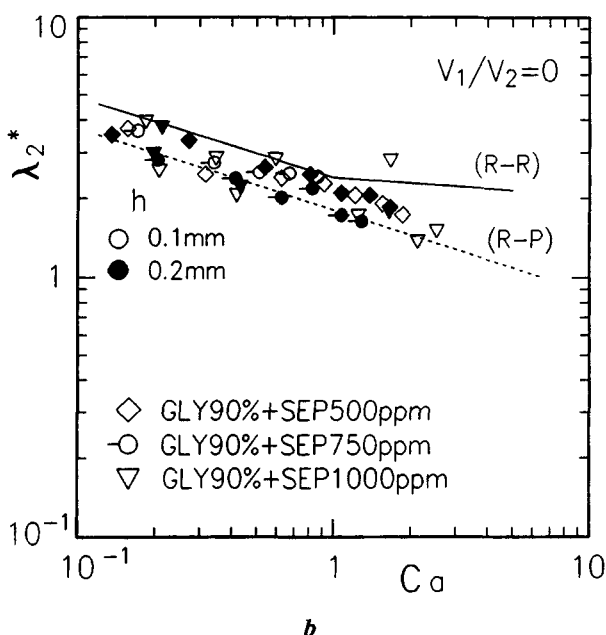
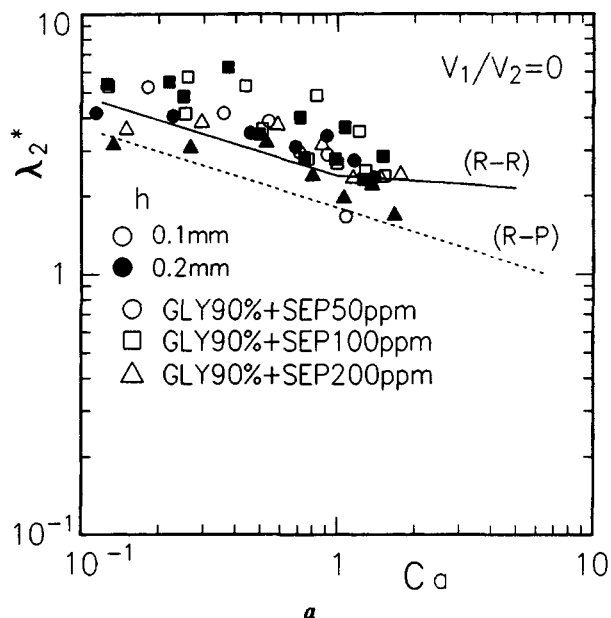


Figure 12. Dimensionless wavelength  $\lambda_2^*$  of ribbing vs. capillary number  $Ca$  for (a) dilute Separan solutions and (b) nondilute Separan solutions.

meniscus generated at the gap exit is brought to the film over the roll, with the wavelength unchanged.

Finally, onset of the ribbing was examined by observing the surface of liquid film over the roll. The result is given in Figure 18 and in the same figure the onset capillary number predicted with the expression by Mill and South (Mill and South, 1967) is also given by dotted lines. It is seen that the predicted values nearly agree with the present experimental data for glycerine

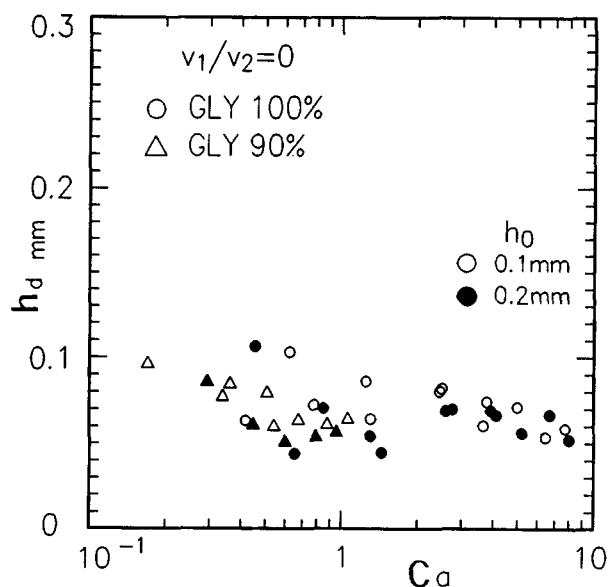


Fig. 13a

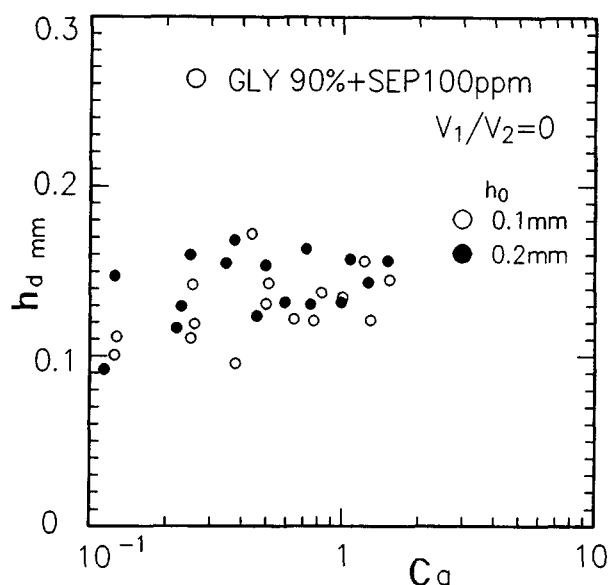


Fig. 13c

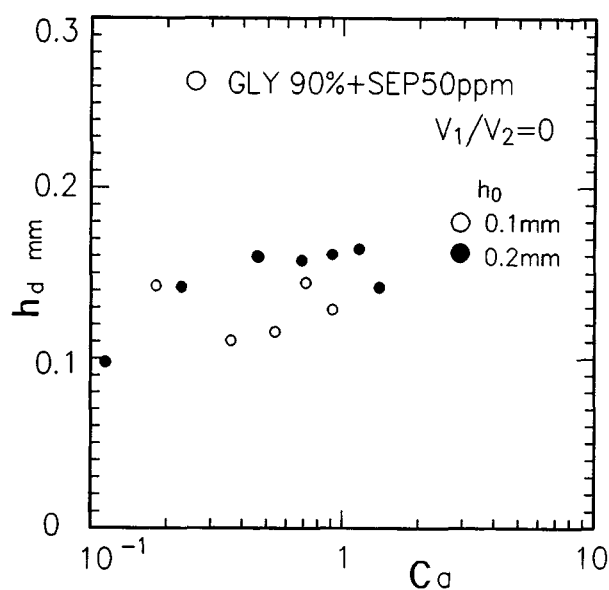


Fig. 13b

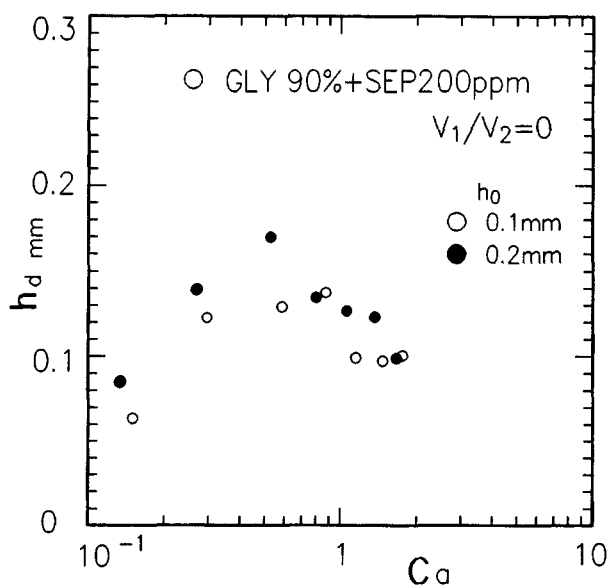


Fig. 13d

solutions and the addition of Separan in glycerine solution promotes the onset of ribbing.

### Elimination of Ribbings

It was mentioned in the previous section that the wavelength of ribbing coincides with that of the deformed meniscus occurring at the gap exit. This suggests that the ribbing originates at the gap exit. Then one may naturally have an idea that ribbings may be controlled by treating the meniscus at the gap exit of rolls. We describe here a simple method of how to eliminate ribbings in the roll coating by the treatment of the meniscus at the gap exit.

Figure 19 shows the method. This time the direction of rotation of the two rolls is reversed (compare Figures 2 and 19). To treat the meniscus of the liquid pool at the gap exit, a string is used. A fishing line made of nylon is used as a string, given tension by hand and spanned in the longitudinal direction near above the gap so as to touch the surface of the liquid pool between the gap. At this stage, the detail of relative position of the string against the gap is not clear because of the hand stretching. However, the experiment shows that the relative position and other dimensions of the string are not important factors for eliminating ribbings. It is inferred that the string suppresses the formation of wavy meniscus at the gap exit and consequently the ribbing is eliminated. Strings used are from 0.098 mm to 0.66 mm in diameter and the gap

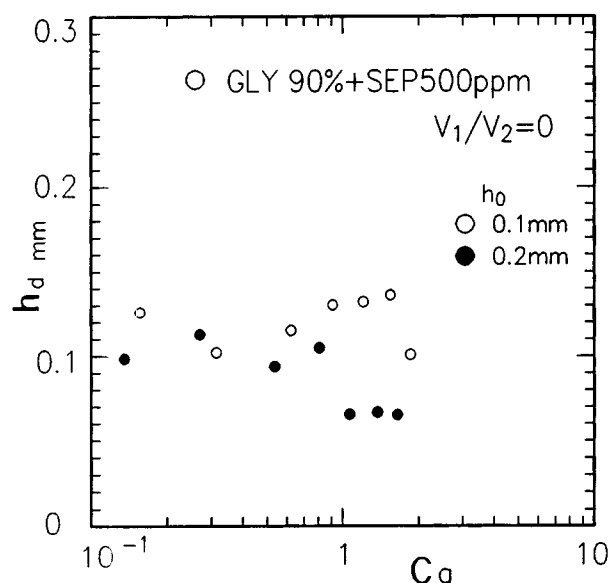


Fig. 13e

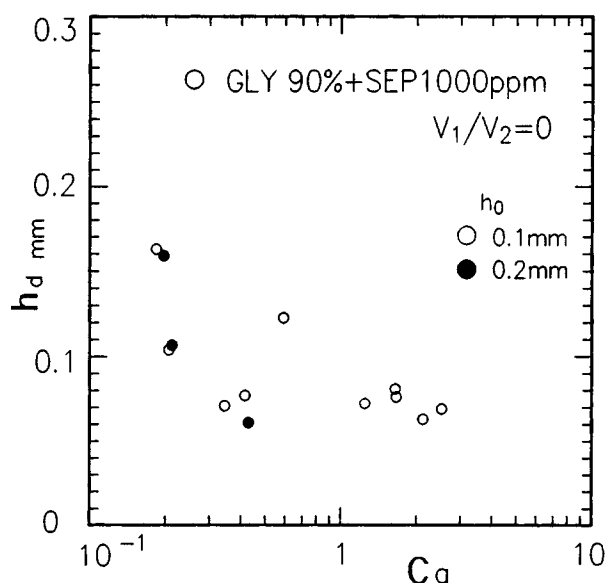


Fig. 13g

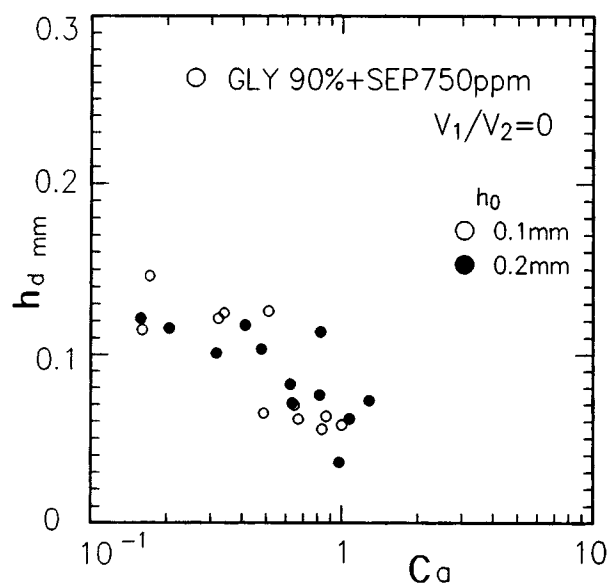


Fig. 13f

Figure 13. Depth  $h_d$  (mm) of ribbing vs. capillary number  $Ca$  for (a) Newtonian liquids and (b)-(g) Separan solutions.

widths are 0.1 mm, 0.2 mm, and 0.3 mm. Liquid tested is glycerine, although the viscosity is 0.418 Pa·s and lower than found usually in a textbook because of the mixture of a small amount of water.

Figures 20 and 21 show examples of the experimental result. Without a string above the gap, ribbings are seen as usual (Figures 20a, 21a). But once a string is set, we have a smooth surface for the same speed of the two rolls (Figures 20b and 20c) and for the different speeds of the two rolls (Figure 21b). According to experiments, this elimination of ribbing is done for various combinations between the speeds of the two rolls and the diameters of the string, but omitted here. It is not obvious how much the setting of a string affects the thickness of the liquid film at the present stage, but this method is very

easy to execute. Therefore this may be available for eliminating ribbings in real coating processes in factories.

## Conclusion

Wavelength and depth of the ribbing occurring in roll coating were measured by a newly developed technique utilizing an image made on the ribbing film surface by a reflection of a straight bar placed above the roll. The following are clarified: Nondimensionalized wavelength is correlated with capillary number for Newtonian liquids, higher for dilute Separan solutions and lower for nondilute Separan solutions than for Newtonian liquids. Depth of ribbing increases for dilute Se-

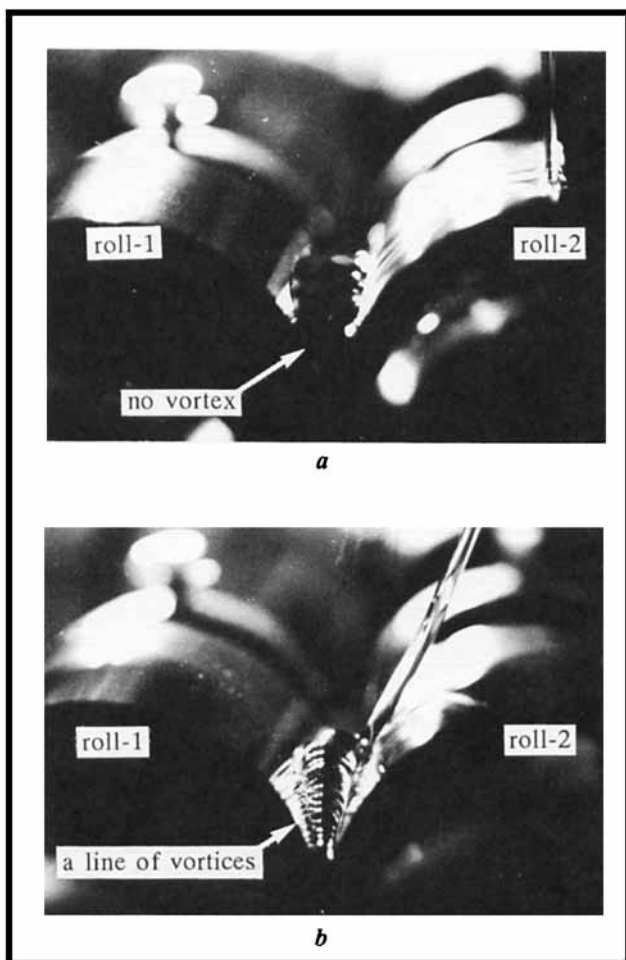


Figure 14. Entrance region of the gap ( $V_2 = 0.254$  m/s,  $h = 0.1$  mm): (a) glycerine 90% + Separan 100 ppm solution; and (b) glycerine 90% + Separan 1,000 ppm solution.

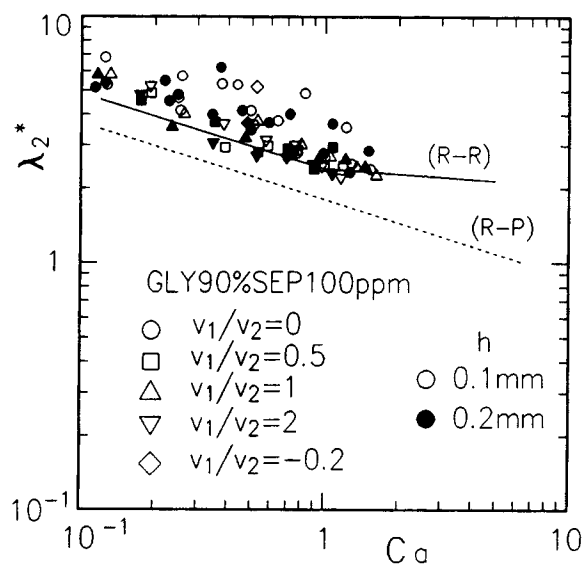


Fig. 15b

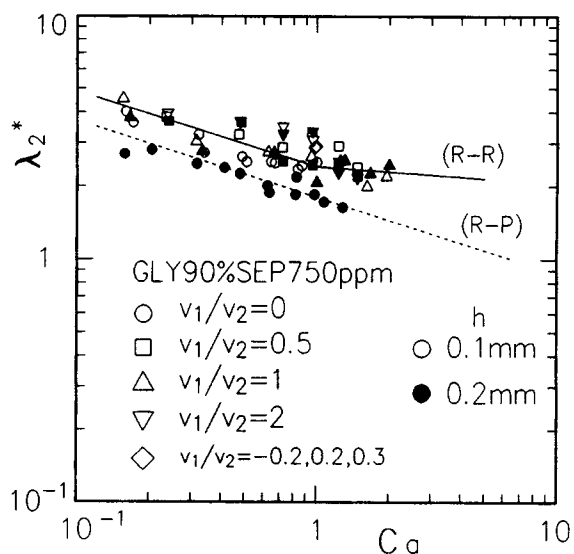


Fig.15c

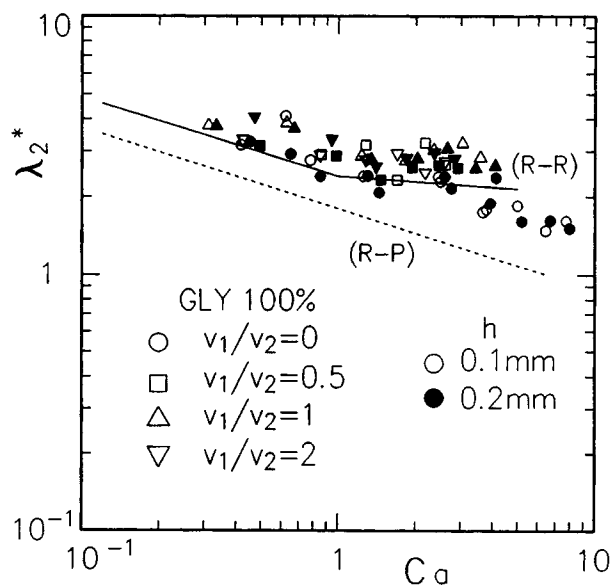


Fig. 15a

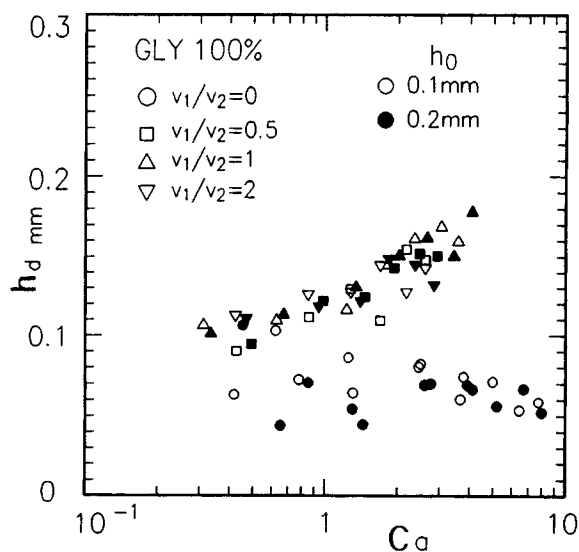


Fig. 15d



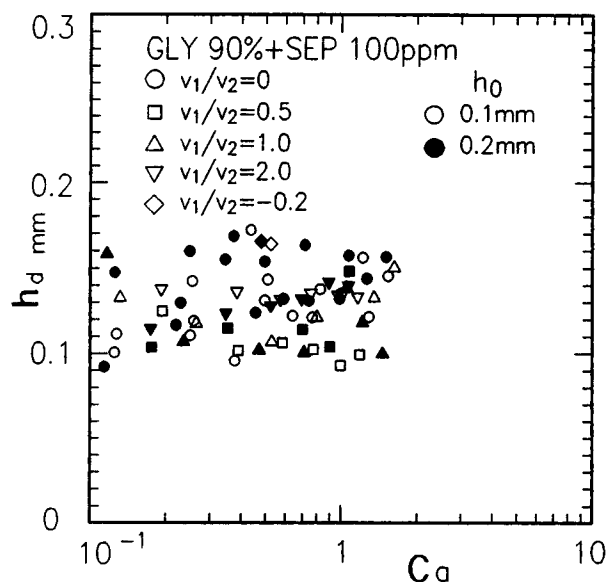


Fig. 15e

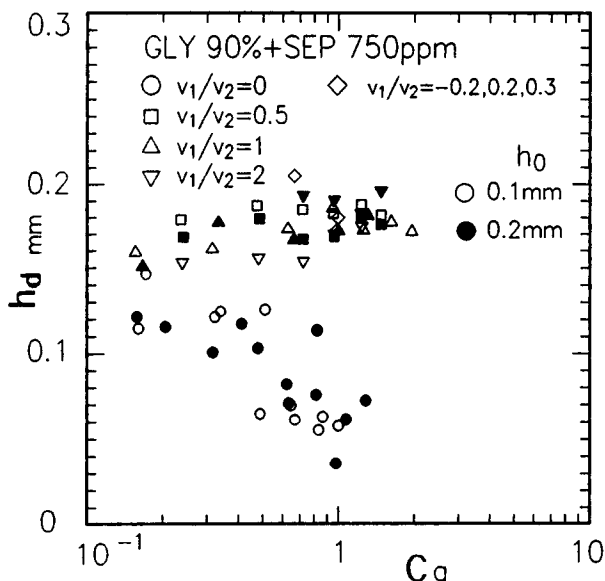


Fig. 15f

Figure 15.  $\lambda_2^*$  and  $h_d$  vs.  $Ca$  in the case of the nonzero velocity of the roll-1, (a) and (d) for glycerine 100%, (b) and (e) for glycerine 90% + Separan 100 ppm solution, (c) and (f) for glycerine 90% + Separan 750 ppm solution.

paran solutions, but it takes nearly the same value for nondilute Separan solutions as those for Newtonian liquid. As a result, we may say that the depth of the ribbing increases with its wavelength. Further, observation revealed that a line of vortices occurs in the entrance region of the gap between the rolls, especially visible for nondilute Separan solutions. These vortices may have some relation to the behavior of the wavelength and the depth of the ribbing and should be studied in the future from this point of view. Increase in the ratio of the velocities

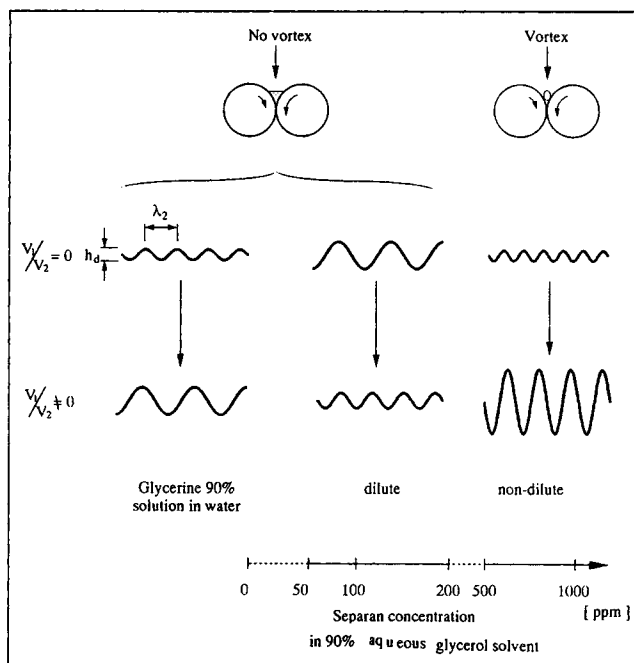


Figure 16. Change in the form of ribbing with increase of Separan concentration.

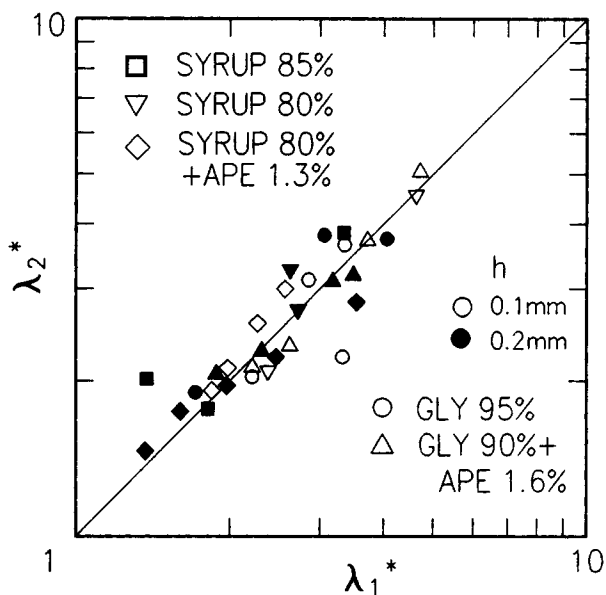
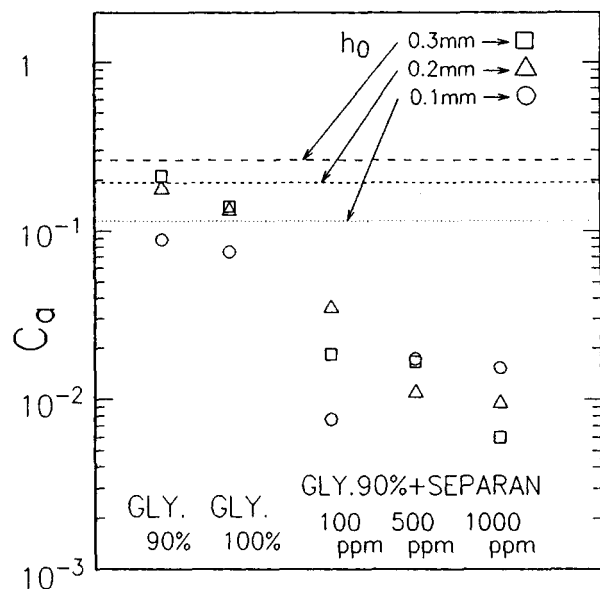


Figure 17. Correlation between  $\lambda_1^*$  and  $\lambda_2^*$ .

of two rolls has an effect to increase both the wavelength and the depth of ribbing for glycerine and nondilute Separan solutions but to decrease them for dilute Separan solutions in comparison of the case where one roll is fixed. Addition of Separan in glycerine solution promotes the generation of ribbing.

A string spanned near over the gap so as to touch the surface of the liquid pool at the gap has an effect to eliminate the ribbing. This is successful in various combinations between the speeds of the two rolls and the diameters of the string.



**Figure 18. Onset of ribbing for various liquids used.**

Dotted lines show the values predicted by the Mill and South's result (Mill and South, 1967).

### Acknowledgment

The authors wish to acknowledge the assistance of Dr. T. Narumi, Mr. M. Konno, Mr. N. Okamoto, Mr. H. Tainaka, Mr. M. Takada and Mr. Y. Takeuchi.

### Notation

$C_a$  = capillary number ( $= \eta v / \sigma$ )

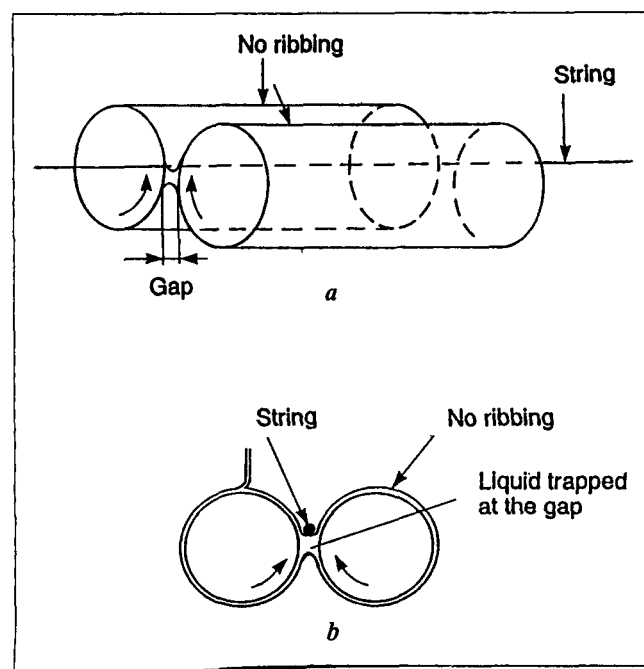


**Figure 19. Method of the present experiment.**

(a) A string is spanned at the gap, being in contact with the liquid trapped between the gap. No ribbing is seen; (b) side view.

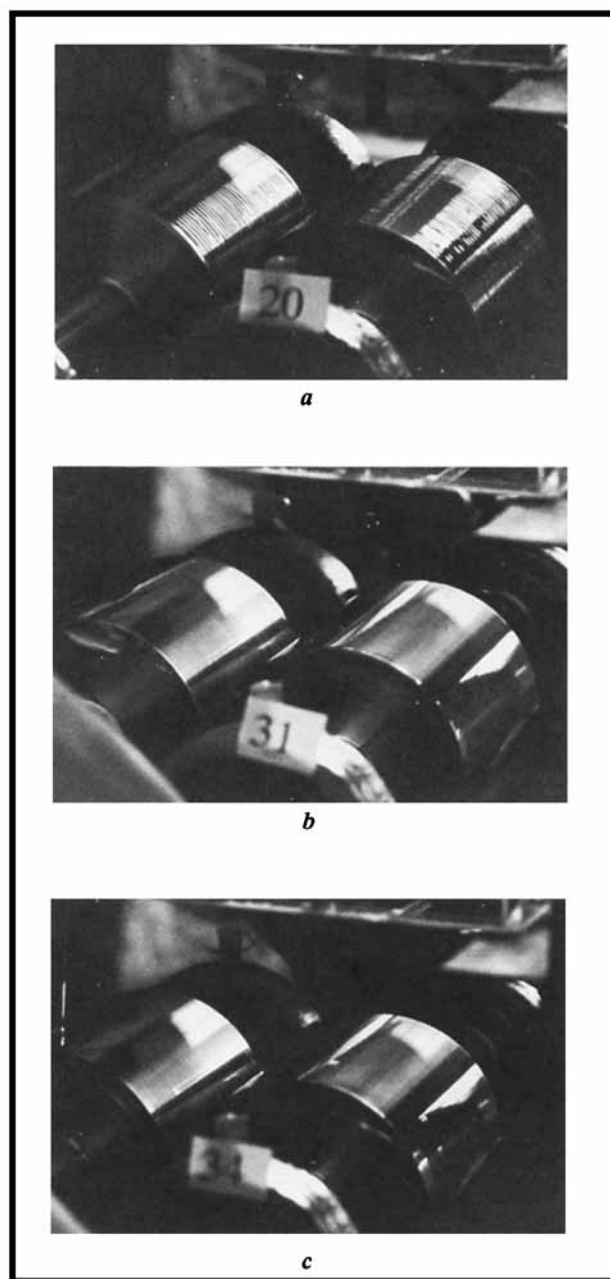


**Figure 20. Elimination of ribbing by means of a string.** The speed of the rolls 1 (right side) and 2 (left side) is the same (0.61 m/s).

The gap is 0.1 mm.

(a) String not set; (b) diameter of the string 0.098 mm; (c) diameter of the string 0.205 mm.

$h$  = gap (or nip) clearance  
 $h_d$  = depth of ribbing of the liquid film  
 $L$  = roll length  
 $R$  = roll radius  
 $v$  = mean velocity ( $= (v_1 + v_2)/2$ )  
 $v_1$  = peripheral velocity of the roll-1  
 $v_2$  = peripheral velocity of the roll-2  
 $\lambda$  = wavelength of the reflection image  
 $Y$  = wave magnitude of the reflection image

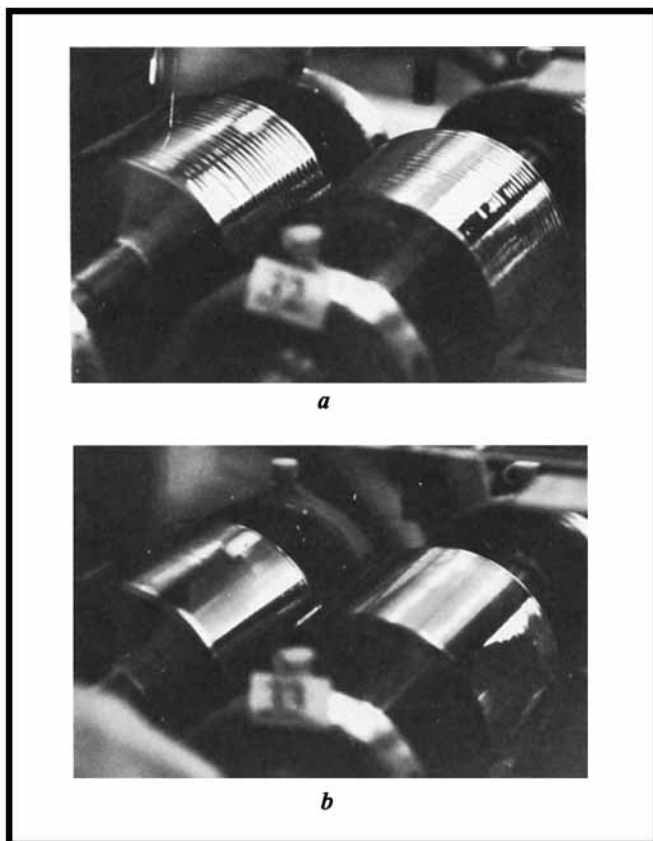


**Figure 21. Elimination of ribbing by means of a string.**

The speeds of the rolls on the left side and on the right side are 1.25 m/s and 0.61 m/s respectively. The gap is 0.3 mm.

(a) String not set; (b) diameter of the string 0.205 mm.

#### Greek letters

$\theta$  = liquid temperature  
 $\eta$  = viscosity

$\lambda_1$  = wavelength of the deformed meniscus at the gap exit  
 $\lambda_1^*$  = dimensionless wavelength of the deformed meniscus ( $= \lambda_1 / (Rh^2)^{1/3}$ )  
 $\lambda_2$  = wavelength of ribbing of the liquid film  
 $\lambda_2^*$  = dimensionless wavelength of rib ( $= \lambda_2 / (Rh^2)^{1/3}$ )  
 $\sigma$  = surface tension

#### Literature Cited

- Adachi, K., "A Hydrodynamics Aspect on Roll Coating," *Tosoh-Kohgaku* (in Japanese), **21**(8), 367 (1986).  
 Babchin, A. J., R. J. Clish, and D. Wahren, "Stability and Disturbance of Coating Films," *Adv. in Colloid and Interf. Sci.*, **14**, 251 (1981).  
 Benkreira, H., M. F. Edwards, and W. L. Wilkinson, "Roll Coating of Purely Viscous Liquids," *Chem. Eng. Sci.*, **36**, 429 (1981).  
 Coyle, D. J., C. W. Macosko, and L. E. Scriven, "The Fluid Dynamics of Reverse Roll Coating," *AIChE J.*, **36**(2), 161 (1990).  
 Coyle, D. J., C. W. Macosko, and L. E. Scriven, "Stability of Symmetric Film-Splitting between Counter-Rotating Cylinders," *J. Fluid Mech.*, **216**, 437 (1990).  
 Coyle, D. J., C. W. Macosko, and L. E. Scriven, "Reverse Roll Coating of Non-Newtonian Liquids," *J. Rheology*, **34**(5), 615 (1990).  
 Mill, C. C., and G. R. South, "Formation of Ribs on Rotating Rollers," *J. Fluid Mech.*, **28**, 523 (1967).  
 Pitts, E., and J. Greiller, "The Flow of Thin Liquid Films Between Rollers," *J. Fluid Mech.*, **11**, 33 (1961).  
 Savage, M. D., "Cavitation in Lubrication. Part 1. On Boundary Conditions and Cavity-Fluid Interfaces," *J. Fluid Mech.*, **80**, 743 (1977).  
 Savage, M. D., "Cavitation in Lubrication. Part 2. Analysis of Wavy Interfaces," *J. Fluid Mech.*, **80**, 757 (1977).  
 Savage, M. D., "Mathematical Model for the Onset of Ribbing," *AIChE J.*, **30**(6), 999 (1984).  
 Sorimachi, K., and T. Hasegawa, "A Study of Torque and Force Working between Two Rolls Lubricated with Liquid," *Trans. of the Japan Soc. of Mech. Eng.*, **57**(542), 3408 (1991).  
 Takemura, Y., K. Adachi, and R. Nakamura, "Study on Coating Flow between Metal Rolls," *Kagaku-Kohgaku Kouen Yohshi Shuh* (in Japanese), **20**, 289 (1987).

Manuscript received Oct. 19, 1992, and revision received Nov. 16, 1992.